Simultaneous connection of Type-3 and Type-4 Off-shore wind farms to HVDC Diode Rectifier Units

R. Vidal-Albalate†, R. Pena‡, E. Belenguer†, S. Añó-Villalba*, S. Bernal-Perez*, R. Blasco-Gimenez*
*Universitat Politècnica de València, Spain (r.blasco@ieee.org)
†Universitat Jaume I de Castelló, Spain
‡Universidad de Concepción, Chile

***Abstract*—This paper introduces a control strategy which can be used for the connection of both type-3 and type-4 wind turbines to HVDC-Diode Rectifier (HVDC-DR) stations. In this way, wind turbines from different technologies could effectively connected to the same HVDC Diode Rectifier station. The proposed strategy is verified by means of PSCAD simulations including start-up operation, optimal power tracking with changing wind conditions and off-shore ac-grid frequency reference changes. Moreover, reactive power sharing between the wind turbines is proven for the aforementioned scenarios.**

I. Introduction

A continuous drive to reduce offshore wind levelized cost of energy (LCoE) is paramount in order to reduce subsidies to offshore wind energy, driving it closer to market prices.

Diode rectifier stations for the connection of large offshore wind power plants (OWPPs) allow for increased efficiency and robustness and can lead to substantial CAPEX and OPEX reduction [1], [2]. The use of diode rectifier stations for the HVDC connection of OWPPs has been proposed for type-4 OWPPs [3], [4], [5], [6], [7]. The authors have also proposed a general solution for the connection of type-3 wind turbines to diode rectifier based HVDC links [8].

It is envisaged that more than one OWPP might be connected to one (or several series connected) diode rectifier units. Therefore, it is important to show that different types of OWPPs can cooperate in the control of the off-shore ac-grid.

This paper extends the results of the control framework already presented in [8] for type-3 wind turbines to obtain a compatible control strategy also applicable to type-4 OWPPs.

The paper covers the detailed description and analysis of the proposed control strategy, as well as simulation studies based on detailed PSCAD models which show the technical feasibility of joint type-3 and type-4 OWPP operation when connected to the same diode rectifier station.

The approach used in this paper consists on using the strategy in [9], [8], which allows the DFIG to behave as an ac voltage source of programmable amplitude and phase.

The off-shore ac-grid is controlled by standard P/f, Q/V droops, which can easily be implemented in the grid side converter of type-4 wind turbines.

The proposed control approach is verified by means of detailed PSCAD simulations. Considered scenarios include start-up operation, optimal power tracking to changing wind conditions and the response of the off-shore ac-grid to changing frequency references.

In all these cases, good reactive power sharing amongst the wind turbines has been verified.

A small signal stability analysis has also been included as a guideline for choosing the droop parameters.

Therefore, this paper will show the technical feasibility of the joint connection of type-3 and type-4 wind turbines to HVDC diode rectifier stations using the same voltage referenced control strategy in both types of wind turbines.

II. Wind turbine control strategy

Figure 1 shows the system under consideration. The 405 MW wind farm consists of 135 wind turbines of 3 MW each, connected to a 66 kV collector bus. The collector bus is connected to a ±300 kV HVDC link by means of a 12-pulse HVDC diode rectifier station. A HVDC-VSC inverter is used for onshore grid connection and for HVDC link voltage control.

The simulated wind farm consists of 5 clusters of 27 wind turbines (81 MW each). The first three clusters consist of DFIG-based wind turbines, whereas cluster 4 and cluster 5 correspond to PMSG-based wind turbines.

A. DFIG-based Wind Turbine Control

The wind turbine dc-link voltage (E_{Dcn}) control is carried out by the wind turbine front-end converter, using standard vector control [9].

The back-end converter is used to control the DFIG using Indirect Stator Flux Orientation (ISFO) [9].

Considering the DFIG dynamic equations in the synchronous rotating $d-q$ frame, we have:

$$\lambda_{ds} = L_s i_{ds} + L_0 i_{dr} \quad (1)$$

$$\lambda_{qs} = L_s i_{qs} + L_0 i_{qr} \quad (2)$$

$$\lambda_{dr} = L_0 i_{ds} + L_r i_{dr} \quad (3)$$

$$\lambda_{qr} = L_0 i_{qs} + L_r i_{qr} \quad (4)$$

$$v_{ds} = R_s i_{ds} + \frac{d\lambda_{ds}}{dt} - \omega_e \lambda_{qs} \quad (5)$$

$$v_{qs} = R_s i_{qs} + \frac{d\lambda_{qs}}{dt} + \omega_e \lambda_{ds} \quad (6)$$

$$v_{dr} = R_r i_{dr} + \frac{d\lambda_{dr}}{dt} - (\omega_e - \omega_r)\lambda_{qr} \quad (7)$$

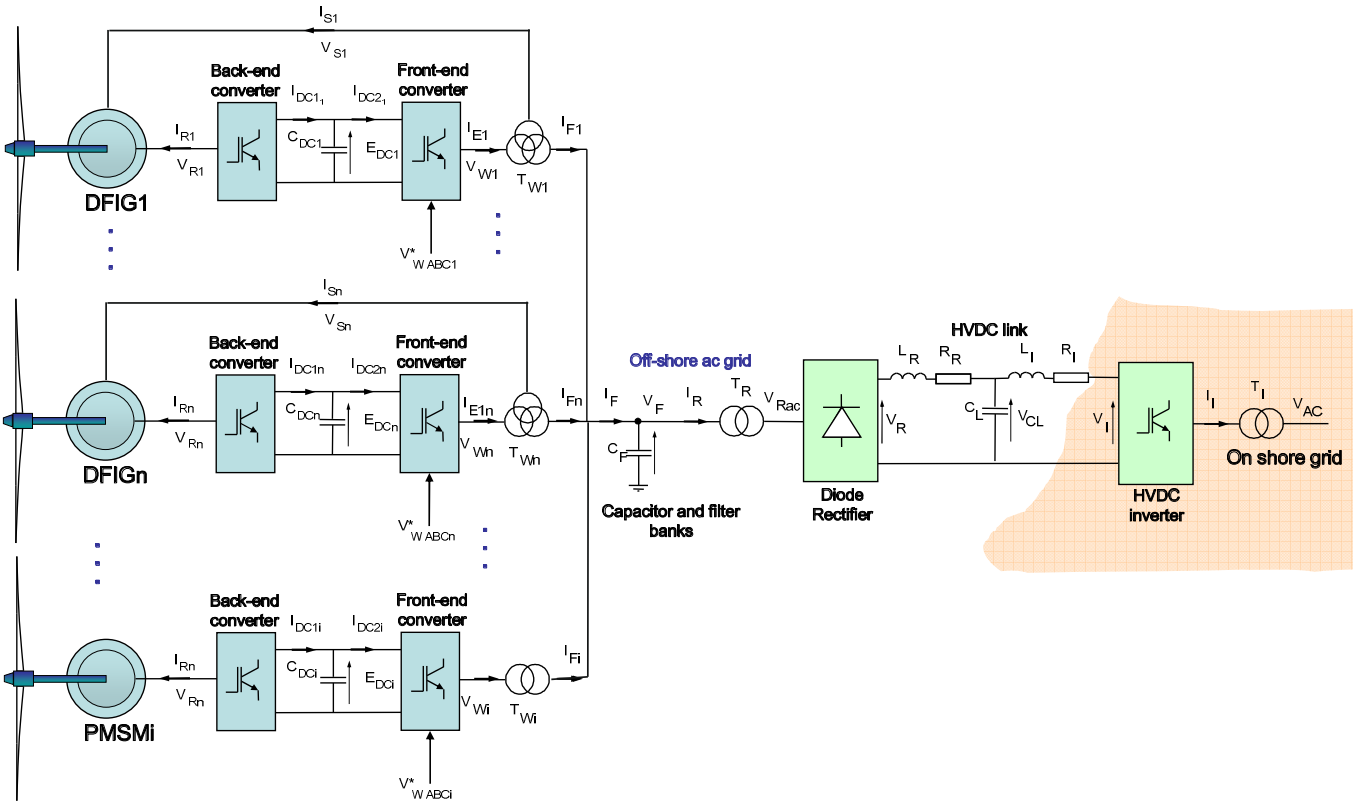

Fig. 1. Mixed DFIG and MPSG-based OWF connected to a HVDC-DR station

$$v_{qr} = R_r i_{qr} + \frac{d\lambda_{qr}}{dt} + (\omega_e - \omega_r)\lambda_{dr} \quad (8)$$

The DFIG is operated using stator field orientation, i.e.:

$$\lambda_{qs} = 0 \quad (9)$$

$$\lambda_{ds} = L_0 i_{ms} \quad (10)$$

where i_{ms} is the stator magnetising current. Therefore equation (2) becomes:

$$i_{qr} = -\frac{L_s}{L_0} i_{qs} \quad (11)$$

Indirect Field Orientation is achived by using the DFIG current control to force (11). Therefore, the quadrature rotor current reference (i^*_{qr}) will be:

$$i^*_{qr} = -\frac{L_s}{L_0} i_{qs} \quad (12)$$

Considering stator flux field orientation and constant stator flux magnitude, eqs. (5) and (6) become:

$$v_{ds} = R_s i_{ds} \quad (13)$$

$$v_{qs} = R_s i_{qs} + \omega_e \lambda_{ds} = R_s i_{qs} + \omega_e L_0 i_{ms} \quad (14)$$

Neglecting the stator resistance voltage drop, the stator voltage can be calculated as:

$$V_s = \sqrt{v_{ds}^2 + v_{qs}^2} \approx V_{emf} = \omega_e L_0 i_{ms} \quad (15)$$

clearly, V_s is proportional to i_{ms}. Therefore, by controlling i_{ms}, it is possible to set the DFIG stator voltage magnitude. The desired magnetising current can be set by using the rotor direct current (i_{dr}) as control action:

$$\tau_{ms} \frac{di_{ms}}{dt} + i_{ms} = i_{dr} + \frac{1+\sigma_s}{R_s} v_{ds} \quad (16)$$

Figure 2 shows the complete diagram for the DFIG control. As shown in this section, the inputs to the proposed control are the desired back-emf magnitude (V^*_{emf}) and phase angle (θ^*_{emf}). Neglecting stator resistance and stator leakage inductance, the stator voltage vector is equal to the stator back-emf, hence the DFIG can be controlled to provide desired stator voltage magnitude and phase (frequency) [9], [8].

B. PMSG-based Wind Turbine Control

The PMSG machine side converter is controlled to keep constant dc-link voltage (E_{Dci}) [6], [7]. In this way, two degrees of freedom can be used for the control fo the grid-side converter.

Previous work by the authors used these two degrees of freedom for the independent control of grid side converter active and reactive power current components (I_{Fdi},I_{Fqi}). However, in this paper, the PMSG grid-side converters are simply set to follow a given voltage magnitude and phase angle reference (V_{Wi}, $\theta_{V_{Wi}}$).

III. Wind power plant control strategy

As both type-3 and type-4 wind turbines can be controlled to follow instantaneous voltage references, a control strategy

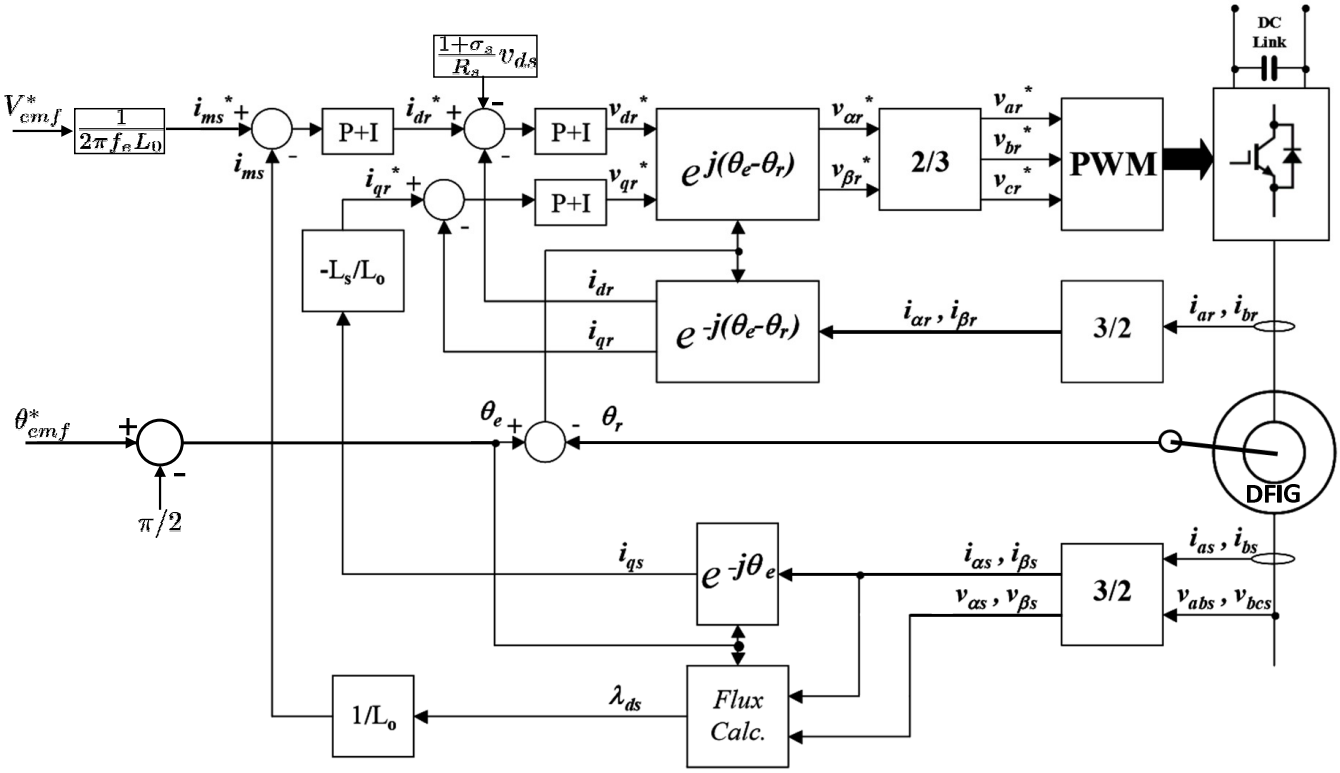

Fig. 2. Voltage referenced DFIG Indirect Stator Flux Orientation Control

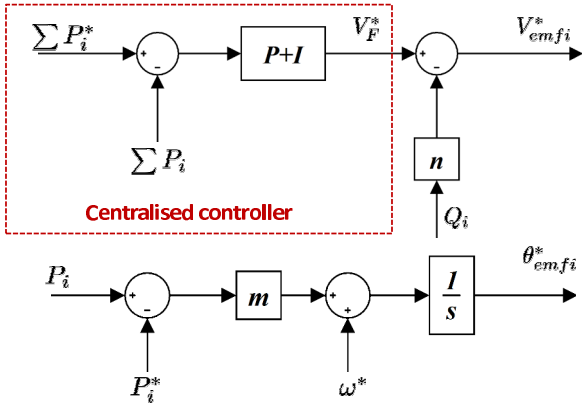

Fig. 3. DFIG WT Control Strategy

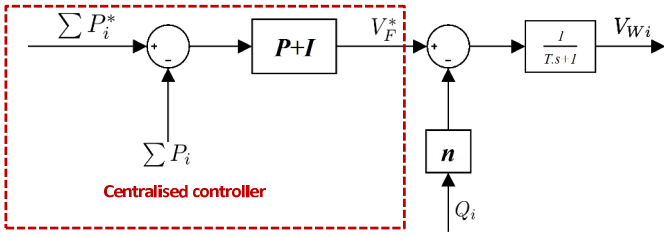

Fig. 4. PMSG WT Control Strategy

based in standard P/f and Q/V droops is used for the control of the off-shore ac-grid:

$$V^*_{emfi} = V^*_F - nQ_i \quad (17)$$

$$\theta^*_{emfi} = \int \{\omega^* - m\,(P^*_i - P_i)\}\,dt \quad (18)$$

where the active power reference of each wind turbine is given by the wind turbine aerodynamic control. For optimum power extraction $P^*_i = k_t\omega_t^3$ below rated speed, where ω_t is the wind turbine rotational speed and k_t is an optimal constant coefficient.

Clearly, if all the droop coefficients are the same, then active and reactive power will be shared equally amongst wind turbines. Figure 3 shows the control strategy used of the DFIGs, including the previously mentioned droops.

The proposed droop control, together with optimal active power references (P^*_i), lead to an active power sharing proportional to the wind resource available in each wind turbine. However, in order to achive maximum optimal power, a centralised secondary controller for the total active power ($\sum P^*_i$) has been included to modify the off-shore grid voltage reference (V^*_F).

However, the response times of the DFIG and the PMSG based wind turbines to changes in stator voltage magnitude are very different. In the case of the DFIG, the back-emf voltage (V^*_{emf}) dynamics are about the same as the rotor current dynamics, and are usually in the order of tens of milliseconds for wind turbines of the considered rating.

On the other hand, grid side converter of a type-4 wind

turbine can deliver desired voltage in one switching period.

Therefore, if PMSG-based wind turbines also use the off-shore ac-grid control strategy shown in 3, then they will be subjected to unequal power sharing during transients.

Therefore, the PMSG-based wind turbines will use the slighly modified control method shown in Fig. 4. In this case the first order lag $\frac{1}{\tau s+1}$ is introduced to make the dynamic response of the PMSGs similar to that of the DFIGs.

Therefore, when the dynamics of both DFIGs and PMSGs based wind turbines are similar, power sharing during transients is improved.

A. Small signal stability

The design and dynamics of standard P/f and Q/V droops is well known. However, the considered system includes a lag, either by design, as in the PMSG, or as a result of the indirect control of the DFIG back-emf.

This section includes the small signal stability analysis for the proposed type-3 and type-4 wind farm control strategy.

The droops used to share the active and reactive powers among the wind turbines are:

$$\omega_{Wi} = \omega^*_{Wi} - mP_{Wi} \tag{19}$$

$$V_{Wi} = V^*_F - nQ_{Wi} \tag{20}$$

The dynamic of type-3 wind turbines is determined by the dynamic of the generator control. However, type-4 wind turbines are connected to the offshore grid through a full ac-ac converter so the dynamic depends mainly on the power electronic converters.

From Fig. 2, the phase angle of the output voltage of the DFIGs can be changed instantanously by setting θ_{emf}. However, the magnitude of the output voltage presents a first order dynamic according to equations (13) and (14). This behavior is clearly different for type-4 turbines, hence, an additional low-pass filter is included in their droops to resemble the DFIG dynamics.

$$\omega_{Wi} = \omega^*_{Wi} - mP_{Wi} \tag{21}$$

$$V_{Wi} = \frac{1}{\tau s+1}\left(V^*_F - nQ_{Wi}\right) \tag{22}$$

where τ is the time constant of the closed loop control of the magnetizing current of the DFIG (see Fig. 3). In this way, the droop constants m and n guarantee the active and reactive power share in steady state, and the low-pass filter assures the different types of wind turbines have similar dynamics.

The active and reactive power delivered to the grid are given by:

$$P_{Wi} = \frac{V_{Wi}V_F}{X_{T_{Wi}}}\sin\phi_{Wi} \tag{23}$$

$$Q_{Wi} = \frac{V_{Wi}V_F\cos\phi_{Wi} - V_F^2}{X_{T_{Wi}}} \tag{24}$$

where V_{Wi} is the output voltage of the converter, V_F the voltage of the off-shore ac grid, ϕ_{Wi} is the phase angle difference between V_{Wi} and V_F, and $X_{T_{Wi}}$ is the output impedance. Here only an inductive impedance is considered since its value is dominated by the leakage reactance of the transformers.

A small-signal analysis taking into account a finite bus approximation is carried out to get the dynamic of ϕ_{Wi} as in [10]:

$$\widehat{p}_{Wi} = \frac{V_F}{X_{T_{Wi}}}\left(\sin\phi_{Wi}\cdot\widehat{e}_{Wi} + E_{Wi}\cos\phi_{Wi}\cdot\widehat{\phi}_{Wi}\right) \tag{25}$$

$$\widehat{q}_{Wi} = \frac{V_F}{X_{T_{Wi}}}\left(\cos\phi_{Wi}\cdot\widehat{e}_{Wi} - E_{Wi}\sin\phi_{Wi}\cdot\widehat{\phi}_{Wi}\right) \tag{26}$$

$$\widehat{\phi}_{Wi} = -\frac{m}{s}p_{Wi} \tag{27}$$

$$\widehat{e}_{Wi} = -\frac{1}{1+\tau s}nq_{Wi} \tag{28}$$

where $\widehat{\ }$ denotes perturbed values and capital letters denote equilibrium point values. From the above equations, the dynamic of ϕ_{wi} is obtained:

$$s^2\widehat{\phi}_{Wi} + \frac{(1+nV_F\cos\phi_{Wi} + V_{Wi}\tau\cos\phi_{Wi})}{\tau}s\widehat{\phi}_{Wi} + \\ + \frac{mV_{Wi}V_F\left(nV_F + X_{T_{Ti}}\cos\phi_{Wi}\right)}{\tau X_{T_{Wi}}}\widehat{\phi}_{Wi} = 0 \tag{29}$$

The values of m and n can be used to obtain the desired closed loop dynamics.

IV. Results

The proposed control strategy has been evaluated by means of detailed PSCAD® simulations, including start-up operation, optimal power tracking and off-shore ac-grid frequency changes.

A. Start-up operation

Figure 5 shows the start-up operation of the off-shore grid. Initially, both the HVDC link and the wind power plant are energised. At this stage, the HVDC-DR station does not conduct.

To connect the wind farm, the off-shore grid voltage magnitude reference is increased until it reaches a sufficiently high voltage so the HVDC diode rectifier starts conducting.

The HVDC-DC station starts conducting at $t = 0.9$s. At this point, the ripple on (V_R) increases, as well as the power being delivered by the diode rectifier (P_{Rdc}).

Figure 5 also shows that, during the transient, the active power is reasonably shared amongst the wind turbines.

Note that the reactive power delivered by the wind turbines ($\sum Q_i$) increase with increasing off-shore ac-grid voltage (V_F). This is expected, as the reactive power produced by the capacitor banks (C_F in Fig. 1) increases with voltage.

It is worth stressing that active and reactive powers are shared between the wind turbines even during transients. The small differences in active power delivered by each wind turbine cluster ($P_{1...5}$) are mainly due to the fact that the wind speed for each case is different.

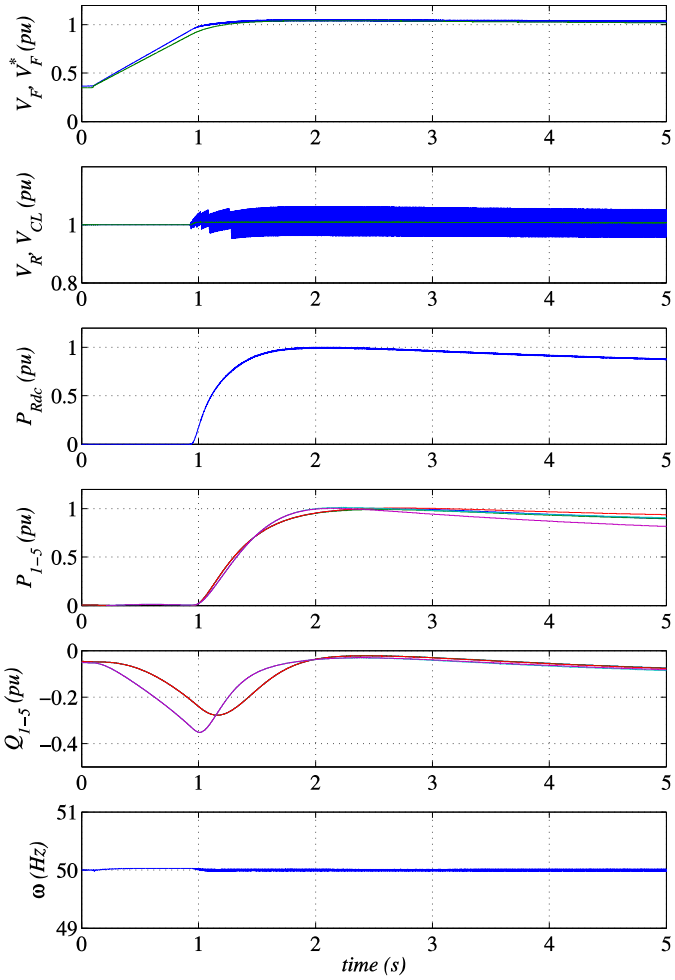

Fig. 5. Start-up operation of the mixed type-3 and type-4 WT wind farm

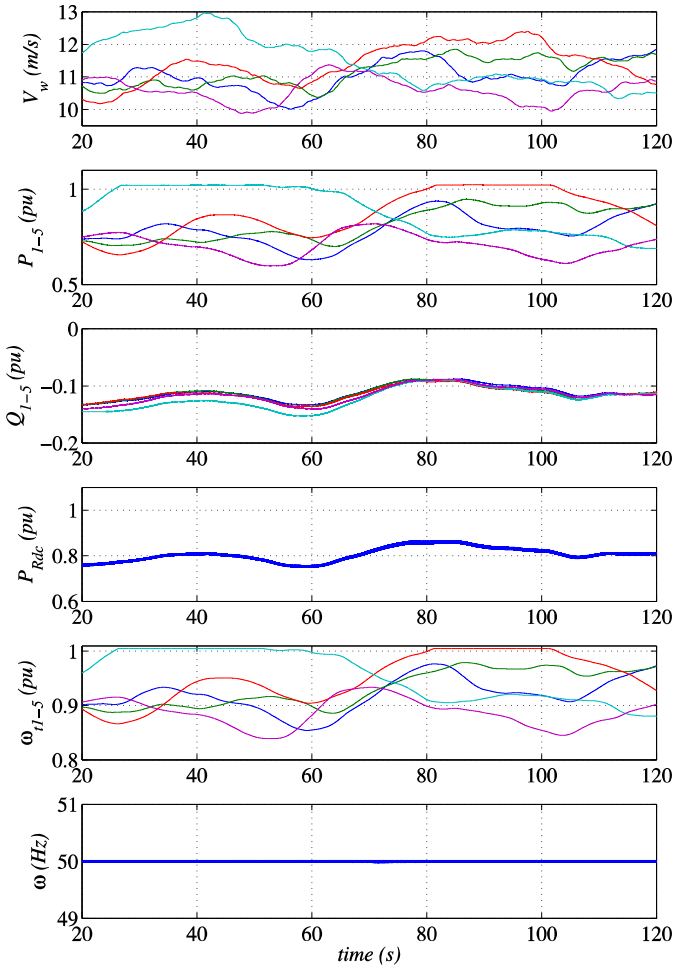

Fig. 6. Optimal power tracking

During the start-up transient, there is a relatively large difference between reactive power being delivered by the DFIGs ($Q_{1...3}$) and that delivered by the PMSGs ($Q_{4,5}$), the latter being slightly faster. This deviation is due to a mismatch between the voltage magnitude dynamics of DFIGs and PMSGs, in spite of the considered first order lag.

Frequency is kept constant during the complete transient.

B. Optimal power tracking

The capability of the proposed control strategy to provide optimal power tracking once the diode rectifier station is conducting is shown in Fig. 6. The top trace shows the average wind speeds for each one of the five clusters. A typical 10% turbulence intensity has been considered whereas wind farm averaging effects have been neglected. Therefore, this assuption will lead to faster active power changes that would otherwise occur in actual installations.

The second trace shows that each wind turbine cluster is delivering its optimal active power reference (P_i^*) even for changing wind conditions. Power limitation by pitch control is also shown here.

The third trace shows a good reactive power sharing amongst the wind turbine clusters, irrespectively of their technology.

The fourth trace shows the averaging effect of the different wind turbine cluster on the power delivered to the HVDC station (P_{Rdc}).

The final two traces of Fig. 6 show the varying wind turbine speeds and also that the off-shore ac-grid frequency is kept constant inspite of the changing delivered power.

It is clearly shown that the proposed control strategy allows for the individual wind turbines to deliver their optimal reference power (P_i^*).

C. Frequency control

The presented control algorithm is also capable of controlling the frequency of the off-shore ac-grid. To illustrate this point, Fig. 7 shows the response to frequency reference changes from 50Hz to 49Hz, then to 51Hz and back to 50Hz.

The second trace of Fig. 7 shows that the off-shore ac-grid voltage is largely unaffected by the changing grid frequency. The same can be said about the active power being delivered by cluster 1 (P_1) and about the power delivered to the HVDC cable (P_{Rdc}).

However, the reactive power delivered by the wind turbines ($Q_{1...5}$) is clearly dependant on the off-shore ac-grid

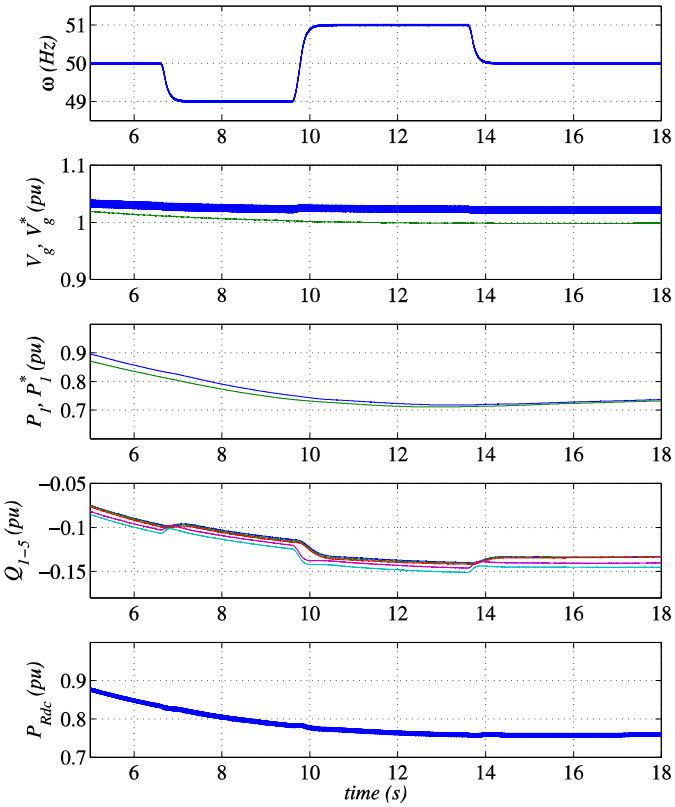

Fig. 7. Variable frequency operation

frequency. Moreover, it is clearly seen that the reactive power is shared reasonably between the 5 wind turbine clusters.

V. Discussion and Conclusions

This paper has shown a control strategy, based on traditional P/f and Q/V droops, for the simultaneous connection of type-3 and type-4 wind turbines to HVDC diode rectifier stations.

A modification on the off-shore ac-grid control strategy for type-4 wind turbines has been introduce in order to equalise voltage magnitude dynamic response between type-3 and type-4 wind turbines.

The proposed control strategy has been verified during simultaneous connection operation, during optimal C_p operation and also during off-shore ac-grid frequency changes.

The study has also shown a good active and reactive power sharing amongst wind turbine clusters even during transients.

Therefore, this study has shown the technical viability of the joint connection of type-3 and type-4 wind turbines to the same HVDC diode rectifier station.

Acknowledgments

The authors would like to thank the support of the Spanish Ministry of Economy and EU FEDER Funds under grant DPI2014-53245-R and Fondecyt Chile under Contract 1151325. The financial support of CONICYT/FONDAP/15110019 and that of the Universitat Jaume I under Grant P1·1B2013-51 is also kindly acknowledged. This project has received funding from the *European Union's Horizon 2020 research and innovation program* under grant agreement No. 691714.

References

[1] Peter Menke, "New Grid Access Solutions for offshore wind farms," *EWEA Off-shore 2015*, Mar. 2015. [Online]. Available: http://www.ewea.org/offshore2015/conference/allposters/PO208.pdf

[2] Peter Menke, Rainer Zurowski, Timo Christ, Slavomir Seman, Gerald Giering, Thomas Hammer, Wolfgang Zink, Felix Hacker, Denis Imamovic, Jan Thisted, Paul Brogan, and Nikolaus Goldenbaum, "Second Generation DC Grid Access for Large Scale Offshore Wind Farms," in *14th International Workshop on Large-Scale Integration of Wind Power into Power Systems as well as on Transmission Networks for Offshore Wind Power Plants*, Brussels, Oct. 2015, pp. 1–6.

[3] S. Bernal-Perez, S. Añó-Villalba, R. Blasco-Gimenez, and J. Rodríguez-D'Derleé, "Efficiency and fault ride-through performance of a diode-rectifier- and VSC-inverter-based HVDC link for offshore wind farms," *Industrial Electronics, IEEE Transactions on*, vol. 60, no. 6, pp. 2401–2409, Jun. 2013.

[4] R. Blasco-Gimenez, N. Aparicio, S. Ano-Villalba, and S. Bernal-Perez, "LCC-HVDC Connection of Offshore Wind Farms With Reduced Filter Banks," *IEEE Transactions on Industrial Electronics*, vol. 60, no. 6, pp. 2372 –2380, Jun. 2013.

[5] S. Bernal-Perez, S. Ano-Villalba, R. Blasco-Gimenez, and N. Aparicio, "Connection of off-shore wind power plants to VSC-MTdc networks using HVdc diode-rectifiers," *Industrial Electronics (ISIE), 2013 IEEE International Symposium on*, pp. 1–6, May 2013.

[6] R. Blasco-Gimenez, S. Añó-Villalba, J. Rodriguez-D'Derlée, S. Bernal-Perez, and F. Morant, "Diode-Based HVdc Link for the Connection of Large Offshore Wind Farms," *Energy Conversion, IEEE Transactions on*, vol. 26, no. 2, pp. 615 –626, Jun. 2011.

[7] R. Blasco-Gimenez, S. Añó-Villalba, J. Rodríguez-D'Derleé, F. Morant, and S. Bernal-Perez, "Distributed voltage and frequency control of offshore wind farms connected with a diode-based HVdc link," *Power Electronics, IEEE Transactions on*, vol. 25, no. 12, pp. 3095–3105, Dec. 2010.

[8] R. Peña, S. Añó-Villalba, and R. Blasco-Gimenez, "Control of DFIG-Based Off-Shore Wind Power Plants for the Connections to HVDC Diode Rectifiers," in *Proc. of the 14th International Workshop on Large-Scale Integration of Wind Power into Power Systems as well as on Transmission Networks for Offshore Wind Power Plants*. Brussels: Energynautics, Oct. 2015.

[9] R. Pena, J. Clare, and G. Asher, "A doubly fed induction generator using back-to-back PWM converters supplying an isolated load from a variable speed wind turbine," *Electric Power Applications, IEE Proceedings* -, vol. 143, no. 5, pp. 380–387, 1996. [Online]. Available: 10.1049/ip-epa:19960454

[10] J. Guerrero, L. de Vicuna, J. Matas, M. Castilla, and J. Miret, "A wireless controller to enhance dynamic performance of parallel inverters in distributed generation systems," *Power Electronics, IEEE Transactions on*, vol. 19, no. 5, pp. 1205–1213, 2004.